喷雾干燥-高温固相法制备纳米 $LiFePO_4$ 与 $LiFePO_4$/C 材料及性能研究

高 飞[1] 唐致远*,[1] 薛建军[2]
([1]天津大学化工学院,天津 300072)
([2]广州鹏辉电池有限公司,广州 511483)

摘要:采用喷雾干燥-高温固相法制备纳米 $LiFePO_4$ 与 $LiFePO_4$/C 正极材料,用 X-射线衍射,扫描电镜等对合成材料进行了表征,并对以 $LiFePO_4$ 为正极的电池进行了电化学性能测试。结果表明:材料合成最佳煅烧温度为 600 ℃;合成过程中由于碳对 $LiFePO_4$ 晶型的生长有一定的抑制作用,相对于纯 $LiFePO_4$ 材料,$LiFePO_4$/C 材料粒径更小;并且,在此最佳合成温度下合成的 $LiFePO_4$/C 正极材料具有良好的电化学性能,在 C/5,1C,5C,10C 等不同倍率放电情况下,首次放电比容量分别为 139.4,137.2,133.5 与 127.3 mAh·g^{-1};表现出良好的循环性能,10C 循环 50 次后,比容量仍保持为 117.7 mAh·g^{-1}(相当于首次放电容量的 92.4%),即每个循环容量衰减仅为 0.15%。

关键词:磷酸铁锂;纳米粒子;喷雾干燥;正极材料
中图分类号:O614.111;TM912.9 **文献标识码**:A **文章编号**:1001-4861(2007)09-1603-06

Preparation and Characterization of Nano-particle $LiFePO_4$ and $LiFePO_4$/C by Spray-drying and Post-annealing Method

GAO Fei[1] TANG Zhi-Yuan*,[1] XUE Jian-Jun[2]
([1]*School of Chemical Engineering and Technology, Tianjin University, Tianjin* 300072)
([2]*Great Power battery Co. Ltd., Guangzhou* 511483)

Abstract: Pure, nano-sized $LiFePO_4$ and $LiFePO_4$/C cathode materials were synthesized by spray-drying and post-annealing method. The crystalline structure, morphology of particles were investigated by X-ray diffraction, scanning electron microscopy. The electrochemical performances of the sample were also measured. The results show that the optimum processing conditions are thermal treatment for 10 h at 600 ℃. Compared with $LiFePO_4$, $LiFePO_4$/C particles are smaller in size due to the inhibition of crystal growth to a great extent by the presence of carbon in the reaction mixture. The $LiFePO_4$/C composite compound is also found to exhibit good electrode properties with discharge capacities of 139.4, 137.2, 133.5 and 127.3 mAh·g^{-1} at C/5, 1C, 5C and 10C rates, respectively. In addition, it shows excellent cycle stability at different current density. Even at a high current density of 10C, the discharge capacity of 117.7 mAh·g^{-1} is obtained (92.4% of its initial value) with only a low capacity fading of 0.15% per cycle.

Key words: $LiFePO_4$; nano-particle; spray-drying; cathode materials

收稿日期:2007-05-21。收修改稿日期:2007-07-02。
广州市科技攻关项目(No.2007Z3-D0021)。
*通讯联系人。E-mail:zytang@tju.edu.cn
第一作者:高 飞,男,29 岁,博士研究生;研究方向:物理化学电源。

Since the first report on the electrochemical properties of $LiFePO_4$ by Goodenough et al.[1], this material is emerging as a promising cathode material for lithium-ion batteries because of low cost and environmental compatibility. In addition, $LiFePO_4$ has a large theoretical capacity of 170 mAh·g^{-1}, a flat discharge potential of 3.4 V vs Li/Li$^+$, a good cycle stability, and an excellent thermal stability. In spite of these attractive features, $LiFePO_4$ requires further modifications to overcome limitations such as poor electronic conductivity and slow lithium ion diffusion. Conductivity is enhanced appreciably by coating $LiFePO_4$ particles with electrically conductive materials like carbon[2~4], metal and metal oxides[5~8]. Minimizing the particle size of $LiFePO_4$ material to provide more surface area has been investigated as a means to enhance ion diffusion[9~11].

To ensure highly homogeneous sub-micro sized particles and pure crystallization, several techniques have been applied to prepare $LiFePO_4$, such as sol-gel, co-precipitation and hydrothermal methods[12~15]. However, these methods have a complex route and high synthetic cost, which restricts their practical application. Therefore, there is still a need to develop a practical synthesis method for preparation of pure, homogeneous $LiFePO_4$ powders with smaller particle size.

The spray-drying method[16,17] has been widely used to synthesize ultra-fine $LiCoO_2$ and sub-sized $LiMn_2O_4$. In this work, nano-particle $LiFePO_4$ and $LiFePO_4$/C cathode materials were synthesized by the spray drying and post-annealing process. The effects of carbon coating and thermal processing conditions on the phase-purity, particle size, morphology and electrochemical performance of the materials are investigated. The cycle performance of lithium cells with these active materials as cathodes is also evalu ated.

1 Experimental

Stoichio metric amounts of $CH_3COOLi \cdot 2H_2O$ (99.9% Sigma-Aldrich), $FeC_2O_4 \cdot 2H_2O$ (98% Sigma-Aldrich) and $(NH_4)_2HPO_4$ (99.5% Sigma-Aldrich) were dissolved in an aqueous solution mixed with polyvinyl alcohol (PVA) (mass ratio of PVA and water being 3∶100). The precursors were then ground for 8 h by wet ball-milling in water solution to decrease the particle size of the reactants and ensure intimate and homogeneous mixing. Finally, a stable suspension was formed. The resulting suspension was dried to form a mixed dry precursor in a spray-dryer. The suspension was atomized via a sprinkler at an air pressure of 0.2 MPa, and was dried in the spray-dryer by hot air. The inlet air temperature was 220 ℃, and the exit air temperature was 110 ℃. The as-prepared precursor powders with pellets ranging from 50 μm to 100 μm were calcined at 300 ℃ for 5 h, and then to the elevated temperatures of 500, 600 and 700 ℃ for 10 h in nitrogen atmosphere. In the end, the samples were reground for 8 h by ball-milling after they were cooled to room temperature. The final products of $LiFePO_4$ were then obtained. For preparing $LiFePO_4$/C, the processing steps were the same as that for $LiFePO_4$ except a mixture of the above raw materials and 5.1wt% of glucose (99.9% Sigma-Aldrich) was used.

The structure and phases of the $LiFePO_4$ and $LiFePO_4$/C thin-film samples were identified by X-ray diffraction (RU-200B/RINT, Rigaku, Rotaflex using monochromatic Cu $K\alpha$ radiation λ=0.154 18 nm, 35 kV, 25 mA, Detector: Scintllation Counter, step scanning: 0.02°). The morphology of the thin-film samples was recorded by using a scanning electron microscopy (Hitachi S800, high vacuum, 10 keV). The specific surface area of the powder particles was measured by the low temperature Nitrogen adsorption and desorption method (Gemini V-2380, N_2-adsorption).

Thin film electrodes were manufactured for electrochemical testing of the samples by casting on an aluminum current collector a *N*-methylpyrrolidone (NMP) slurry of the $LiFePO_4$ active material (82wt%) mixed with a carbon black (Super P-Timcal) conductive additive (10wt%) and a polyvinylidene fluoride (Kyner2801-Eif Atochem) binder (8wt%). These film-type $LiFePO_4$ electrodes were assembled in a nitrogen filled glove box using mesocarbon microbeads (MCMB) anode as a counter electrode. The electrolyte

was 1mol·L^{-1} $LiPF_6$ in a mixture of ethylene carbonate (EC) and diethyl carbonate (DMC) (1∶1, *V*/*V*). The cells were charged and discharged over a voltage range of 2.0~4.2 V.

The electrochemical impedance spectroscopy (EIS) and Cyclic voltammetry (CV) measurements were performed using a voltalab system with VM4 (Radiometer Analytical SAS. PGZ301). These tests were performed using a three-electrode cell. The thin film electrodes of $LiFePO_4$ were used as working electrodes. The counter and reference electrodes were lithium foil. The amplitude of the AC signal of the EIS was 10 mV with the frequency range between 100 kHz and 0.01 Hz. The CV measurements were carried out between 2.5 V and 4.0 V at a scan rate of 0.1 mV·s^{-1}.

2 Results and discussion

Fig.1 shows the effect of calcination temperature on the XRD patterns of $LiFePO_4$ and $LiFePO_4$/C. The samples were prepared by calcining for 10 h at 500, 600 and 700 ℃, respectively. By increasing post-calcination temperature up to 500 ℃, an impurity phase (marked by arrow in Fig.1) appears due to iron (Ⅱ, Ⅲ) pyrophosphates or phosphates (perhaps $Li_3Fe_2(PO_4)_3$ or Li_3PO_4), and when the calcination temperature increases to 600 or 700 ℃, all the diffraction peaks can be indexed on the orthorhombic structure with the space group *Pnmb* and there are no impurity phase peaks. The characteristic peaks of $LiFePO_4$ are formed at the temperature of 600 ℃, which is close to the reported crystallization temperature of ~567 ℃ for $LiFePO_4$[18].

The lattice parameters and the calculated grain size (D_{131}) based on the (131) diffraction peaks for six samples are summarized in Table 1. The grain size was calculated using the Scherer formula. Though the lattice parameters of all the samples have almost the same values, the D_{131} values of $LiFePO_4$ prepared at 500, 600 and 700 ℃ are 38, 49 and 75 nm, respectively, and 32 nm, 41 nm and 56 nm for the corresponding $LiFePO_4$/C samples. It is found that the grain size increases with calcination temperature and the grain size of the $LiFePO_4$/C sample is smaller than that of the corresponding $LiFePO_4$ sample, which confirms that carbon inhibits the crystal growth to a considerable extent.

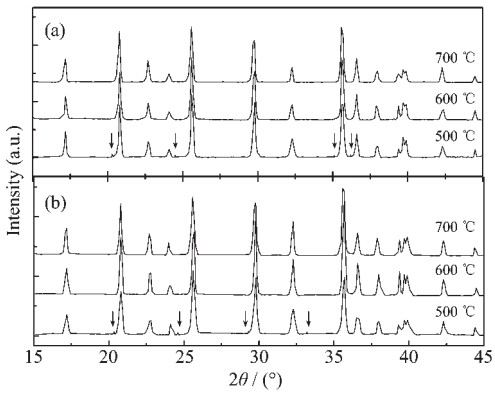

Fig.1　XRD patterns of (a) $LiFePO_4$, (b) $LiFePO_4$/C samples prepared at different temperatures

Fig.2 shows SEM images of the powders. Near-spherical, nano-meter sized particles with minimal agglomeration are obtained for both $LiFePO_4$ and $LiFePO_4$/C. The particle sizes (estimated from SEM analysis, given in Table 1) of the $LiFePO_4$ samples obviously increase with calcination temperature from 90~230 nm at 500 ℃, 120~350 nm at 600℃ to 150~800 nm at 700 ℃. Compared with $LiFePO_4$, $LiFePO_4$/

Table 1　Lattice parameters, calculated grain size (D_{131}) of the (131) diffraction peaks and particle size range for $LiFePO_4$ and $LiFePO_4$/C samples prepared at 500 ℃, 600 ℃ and 700 ℃

Samples	Calcination temperature / ℃	Lattice parameters			Grain size D_{131} / nm	Particle size / nm
		a / nm	*b* / nm	*c* / nm		
$LiFePO_4$	500	1.032	0.599 6	0.468 9	38	90~230
	600	1.031	0.599 8	0.468 7	49	120~350
	700	1.031	0.600 1	0.468 6	75	150~800
$LiFePO_4$/C	500	1.031	0.600 1	0.469 1	32	80~170
	600	1.032	0.600 2	0.468 8	41	80~300
	700	1.032	0.600 2	0.468 7	56	100~500

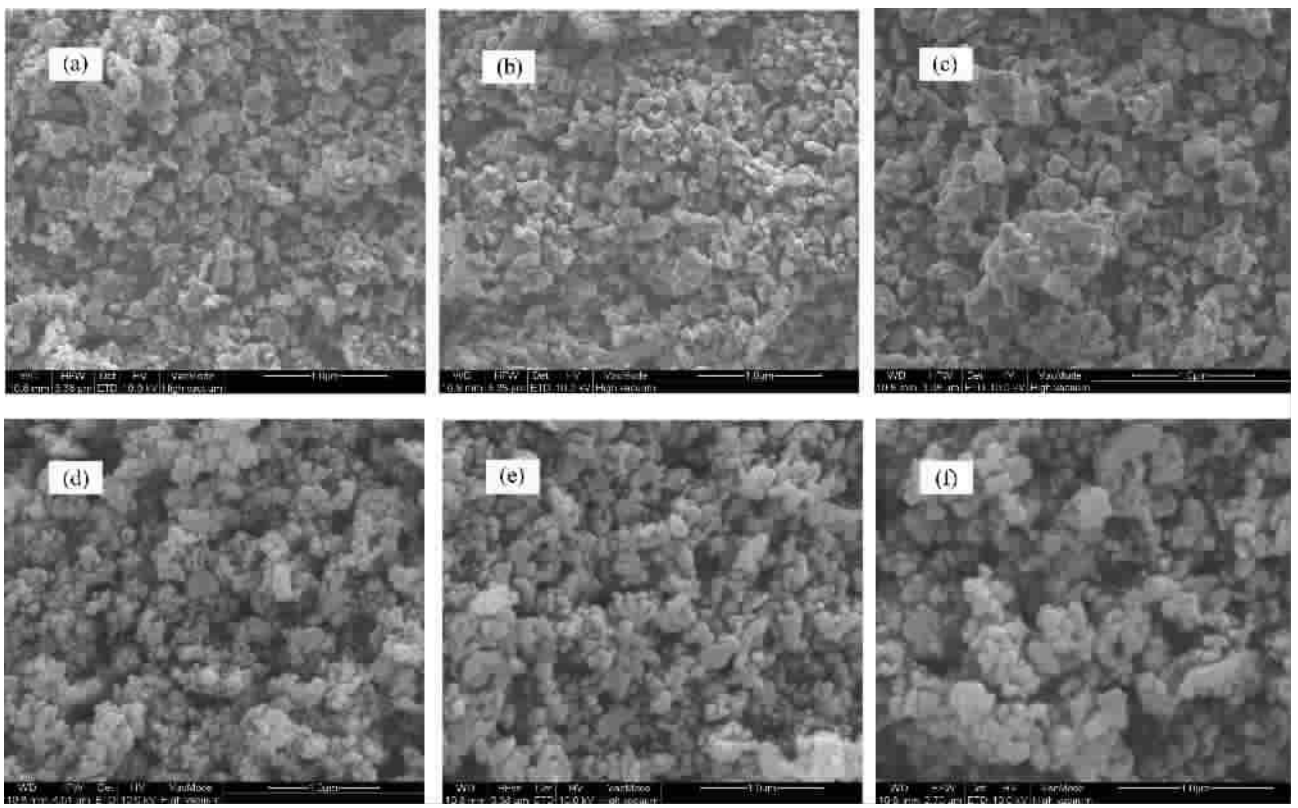

Fig.2 SEM images of samples prepared at different temperatures (a)~(c) $LiFePO_4$ at 500, 600 and 700 ℃, respectively; (d)~(f) $LiFePO_4$/C at 500, 600 and 700 ℃, respectively

C particles are smaller in size due to the inhibition of crystal growth to a great extent by the presence of carbon in the reaction mixture. Generally, an increase in calcination temperature increases the surface area, and the carbon coating in $LiFePO_4$/C provides a comparatively rougher surface texture for the particles. The BET specific surfacearea of the $LiFePO_4$/C samples prepared at 500, 600 and 700 ℃ is 23, 20 and 14 $m^2 \cdot g^{-1}$, respectively.

The electrochemical performance in terms of the initial charge-discharge capacities of $LiFePO_4$ and $LiFePO_4$/C prepared at different calcination temperatures are compared in Fig.3. The $LiFePO_4$/MCMB batteries were measured at room temperature and at the rate of C/5. All the samples exhibit a flat voltage plateau at ~3.3 V, which is the main characteristic of the two-phase reaction in the electrode. The discharge capacities for $LiFePO_4$ prepared at 500, 600 and 700 ℃ are 86.2, 124.5 and 110.6 $mAh \cdot g^{-1}$, respectively, and 113.1, 139.4 and 132.5 $mAh \cdot g^{-1}$ for the corresponding $LiFePO_4$/C samples. $LiFePO_4$/C with conductive carbon coating exhibits higher performance compared with uncoated counterparts. The optimum temperature is 600 ℃ for preparation of samples with smaller particles and more uniform morphology. The performance of the 500 ℃ sample is the poorest, although it has a particle size comparable with that of the 600 ℃ sample. The poorer performance of the 500 ℃ sample could be due to its lower level of crystallinity. The larger particles of the 700 ℃ sample also result in a

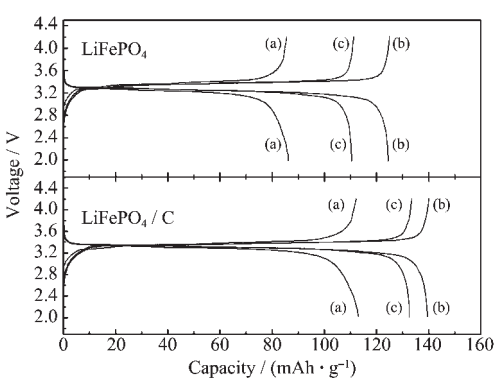

Fig.3 Initial charge and discharge capacities of $LiFePO_4$ and $LiFePO_4$/C samples prepared at (a) 500 ℃, (b) 600 ℃ and (c) 700 ℃ with C/5 rate

poorer performance than the 600 ℃ sample with the optimized particle size and purity level.

Fig.4 shows the Nyquist plots of the electrodes of $LiFePO_4$ and $LiFePO_4$/C obtained at 600 ℃. An intercept at the Z' axis in high frequency corresponds to the ohmic resistance (R_e), which represents the resistance of the electrolyte. The semicircle in the high frequency range indicates the charge transfer resistance (R_{ct}). The inclined line in the lower frequency represents the Warburg impedance (Z_w), which is associated with lithium-ion diffusion in the $LiFePO_4$ particles. Obviously, the resistance R_e is similar for bare $LiFePO_4$ and $LiFePO_4$/C electrodes. This is because that the concentrations of the electrolytes and distances of the three electrodes are the same. The $LiFePO_4$/C electrode exhibits much lower R_{ct} than that of the bare $LiFePO_4$, indicating that the carbon-coating significantly increases the electrical conductivity between $LiFePO_4$ particles. Therefore, the carbon-coating can facilitate the charge-transfer reaction of $LiFePO_4$ electrodes.

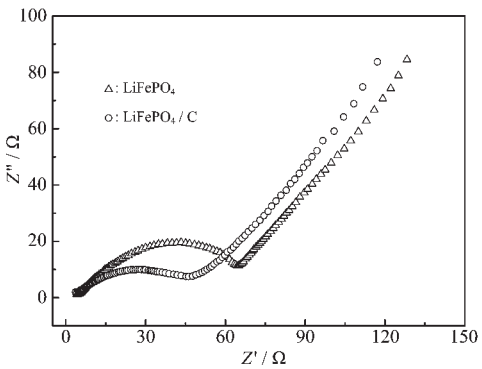

Fig.4　EIS patterns of the electrodes of $LiFePO_4$ and $LiFePO_4$/C obtained at 600 ℃

Further studies have been undertaken with $LiFePO_4$/C prepared at the optimum temperature of 600 ℃. Fig.5 shows Cyclic-voltammetry (CV) for $LiFePO_4$/C film /$LiPF_6$ +EC +DMC/Li cell cycled between 2.5 and 4.0 V versus Li^+/Li at a scan rate of 0.1 mV·s^{-1}. During the anodic sweep, lithium ions are extracted from the $LiFePO_4$ structure. An oxidation peak is located at 3.562 V vs Li/Li^+. When the potential is scanned from 4.0 to 2.5 V, a reduction peak occurrs at 3.246 V, corresponding to lithium insertion into the $LiFePO_4$ structure. After 10 scanning cycles, the redox peaks remain a similar magnitude, indicating good stability of the electrode.

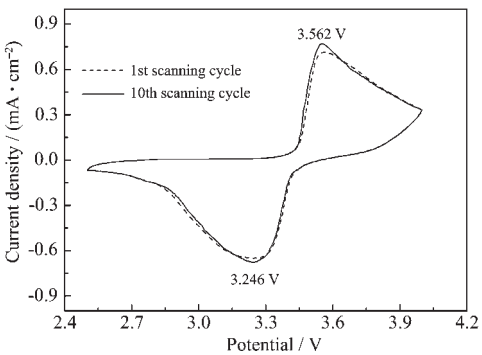

Fig.5　CV curves of $LiFePO_4$/C electrodes in 1 mol·L^{-1} $LiPF_6$/(EC + DEC) at scan rate of 0.1 mV·s^{-1}

The electrochemical rate performance and cycle-ability of $LiFePO_4$/C are shown in Figs.6 and 7. With the increase in current density, the discharge capacity and the plateau voltage are rapidly reduced. At C/5, we can obtain the initial discharge capacity of 139.4 mAh·g^{-1}, while at 1C rate, the capacity is still 137.2 mAh·g^{-1} and for more severe conditions, we have, respectively, 133.5 and 127.3 mAh·g^{-1} at 5C and 10C. A decrease in initial discharge capacity with current density results from the intrinsic lithium ion diffusion limitations of the material. Nevertheless, a good cycling property is shown at different current densities. The capacity retention of $LiFePO_4$/C is almost 100% after 50 cycles at C/5 rate, and a discharge capacity of 117.7 mAh·g^{-1} is obtained (92.4% of its initial value) even after 50 cycles at a high current density of 10C with only a low capacity fading of 0.15% per cycle. In comparison to the results reported

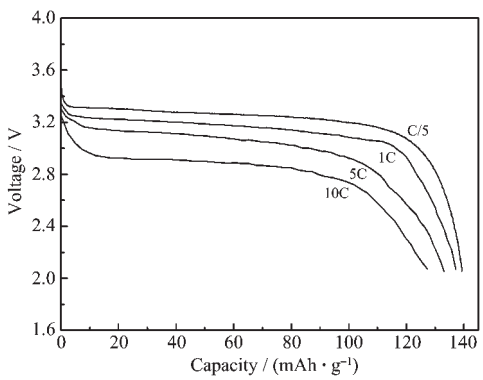

Fig.6　Discharge curves of lithium-ion batteries with $LiFePO_4$/C cathodes at C/5, 1C, 5C and 10C rates

by other research groups in Table 2, the nano-sized $LiFePO_4/C$ composite synthesized via the spray drying method exhibits comparable discharge capacities even at higher rates in our experiments. It is considered that the smaller particle size and intimate contact of the $LiFePO_4$ particles with carbon would result in a relatively superior cyclability and rate capability.

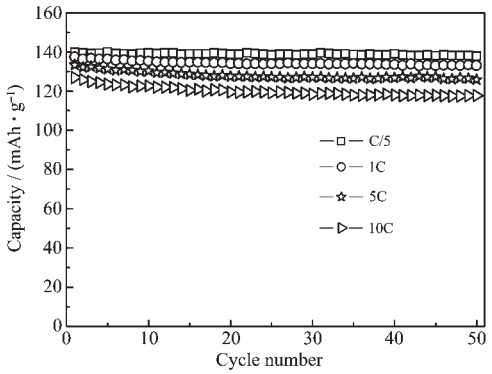

Fig.7 Cycle performance of lithium-ion batteries with $LiFePO_4/C$ cathode at C/5, 1C, 5C and 10C rates

Table 2 Discharge capacities at the high current densities from different sources of $LiFePO_4/C$

$LiFePO_4/C$	Rate	Capacity / ($mAh \cdot g^{-1}$)
Franger S, et al.[3]	5C	125
Meligrana G, et al.[13]	10C	115
Dominko R, et al.[15]	5C	120
Our samples	5C	132
	10C	127

3 Conclusions

Spray-drying and post-annealing method was used to synthesize nano-sized $LiFePO_4$ and $LiFePO_4/C$ cathode materials. The optimum processing conditions are found to be thermal treatment for 10 h at 600 ℃. Compared with $LiFePO_4$, the carbon coating $LiFePO_4/C$ prepared under these optimized conditions displays better performance and exhibits initial discharge capacities of 139.4, 137.2, 133.5 and 127.3 $mAh \cdot g^{-1}$ at C/5, 1C, 5C and 10C rates, respectively. In addition, it shows excellent cycle stability at different current densities. Even at the high current density of 10C, a discharge capacity of 117.7 $mAh \cdot g^{-1}$ is obtained (92.4% of its initial value) with only a capacity fading of 0.15% per cycle.

References:

[1] Padhi A K, Nanjundaswamy K S, Goodenough J B. *J. Electrochem. Soc.*, **1997**,**144**:1188~1194

[2] Bewlay S L, Konstantinov K, Wang G X, et al. *Mater. Lett.*, **2004**,**58**:1788~1791

[3] Franger S, Benoit C, Bourbon C, et al. *J. Phys. Chem. Solids*, **2006**,**67**:1338~1342

[4] Belharouak I, Johnson C, Amine K. *Electroche. Commun.*, **2005**,**7**:983~988

[5] Park K S, Son J T, Chung H T, et al. *Solid State Commun.*, **2004**,**129**:311~314

[6] Ni J F, Zhou H H, Chen J T, et al. *Mater. Lett.*, **2005**,**59**:2361~2365

[7] Liu H, Cao Q, Fu L J, et al. *Electrochem. Commun.*, **2006**,**8**:1553~1557

[8] YING Jie-Rong, LEI Min, JIANG Chang-Yin, et al. *J. Power Sources*, **2006**,**158**:543~549

[9] Arnold G, Garche J, Hemmer R, et al. *J. Power Sources*, **2003**,**119~121**:247~251

[10]Lee J, Teja A S. *Mater Lett.*, **2006**,**60**:2105~2109

[11]Singhal A, Skandan G, Amatucci G, et al. *J. Power Sources*, **2004**,**129**:38~42

[12]Sanchez M A E, Brito G E S, Fantini M C A, et al. *Solid State Ionics*, **2006**,**177**:497~500

[13]Meligrana G, Gerbaldi C, Penazzi N. *J. Power Sources.*, **2006**,**160**:516~522

[14]Needham S A, Calk A, Wang G X, et al. *Electrochem. Commun.*, **2006**,**8**:434~438

[15]Dominko R, Bele M, Gaberscek M, et al. *J. Power Sources*, **2006**,**153**:274~280

[16]Tu J P, Wu H M, Zhang W K. *Mater. Lett.*, **2007**,**61**:864~867

[17]Decheng Li, Yasuhiro Kato, Yuichi Sato. *J. Power Sources*, **2006**,**160**:1342~1348

[18]Scaccia S, Carewska M, Wisniewski P, et al. *Mater. Res. Bull.*, **2003**,**38**:1155~1160